

Regge phenomenology of the N^* and Δ^* poles



Instituto de
Ciencias
Nucleares
UNAM



M. en C. Jorge Antonio Silva-Castro
Universidad Nacional Autónoma de México

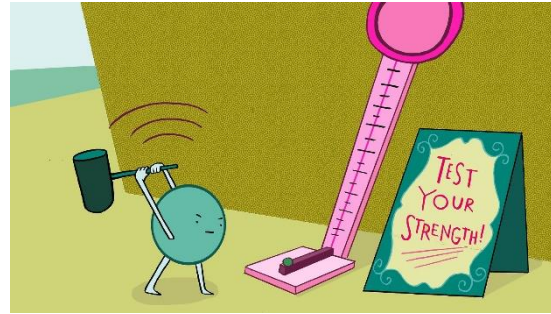
4th Workshop on Future Directions in Spectroscopy Analysis
(FDSA2022)

Outline

- *Physical motivation*
- *Theoretical framework*
- *Poles and models*
- *Results*
- *Conclusions*

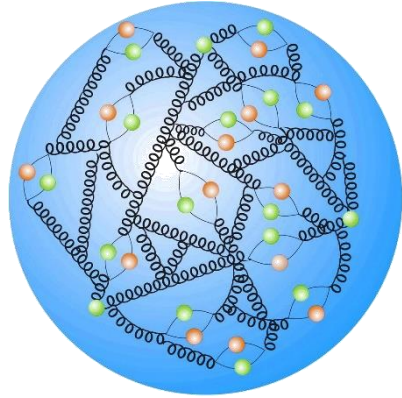
The Strong Interaction

Fundamental force described by QCD



The Strong Interaction

Fundamental force described by QCD

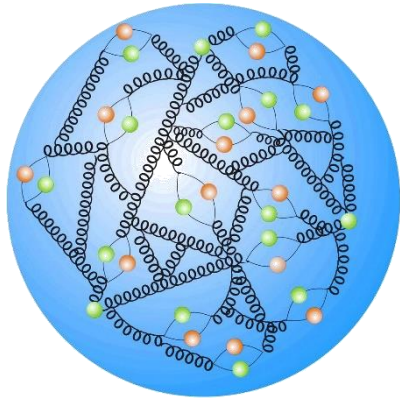


Quarks and gluons are confined in hadrons in color singlets.

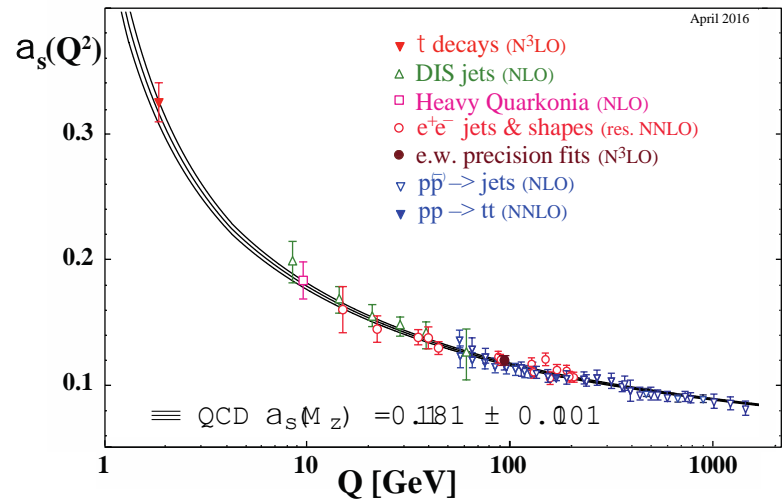
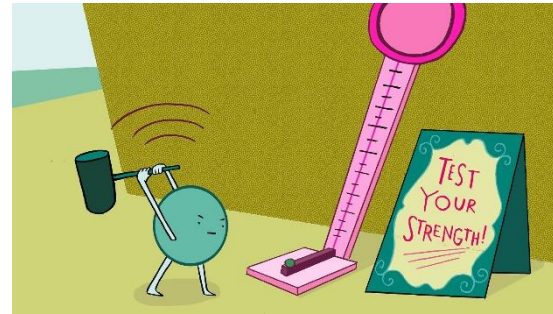


The Strong Interaction

Fundamental force described by QCD

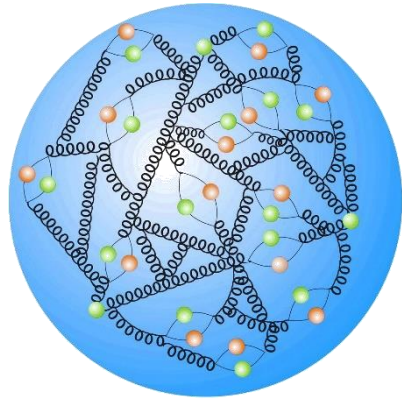


Quarks and gluons are confined in hadrons in color singlets.



The Strong Interaction

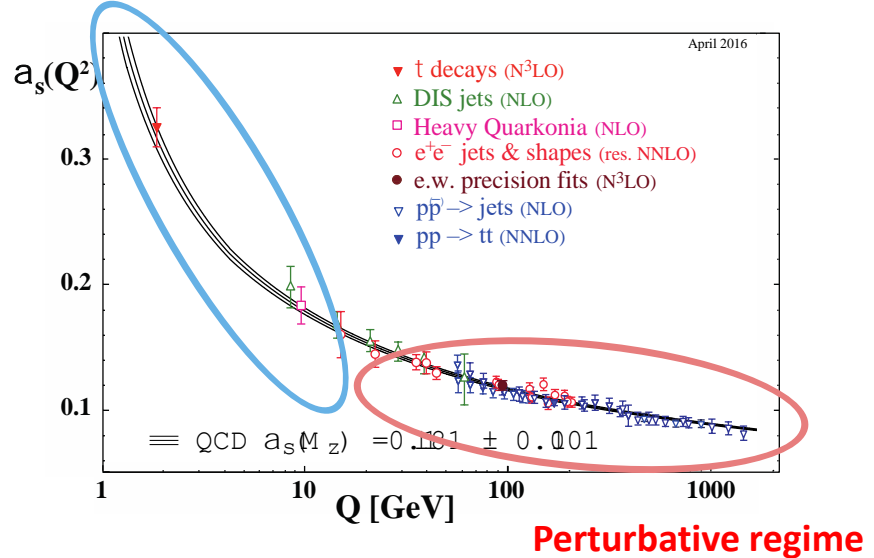
Fundamental force described by QCD



Quarks and gluons are confined in hadrons in color singlets.



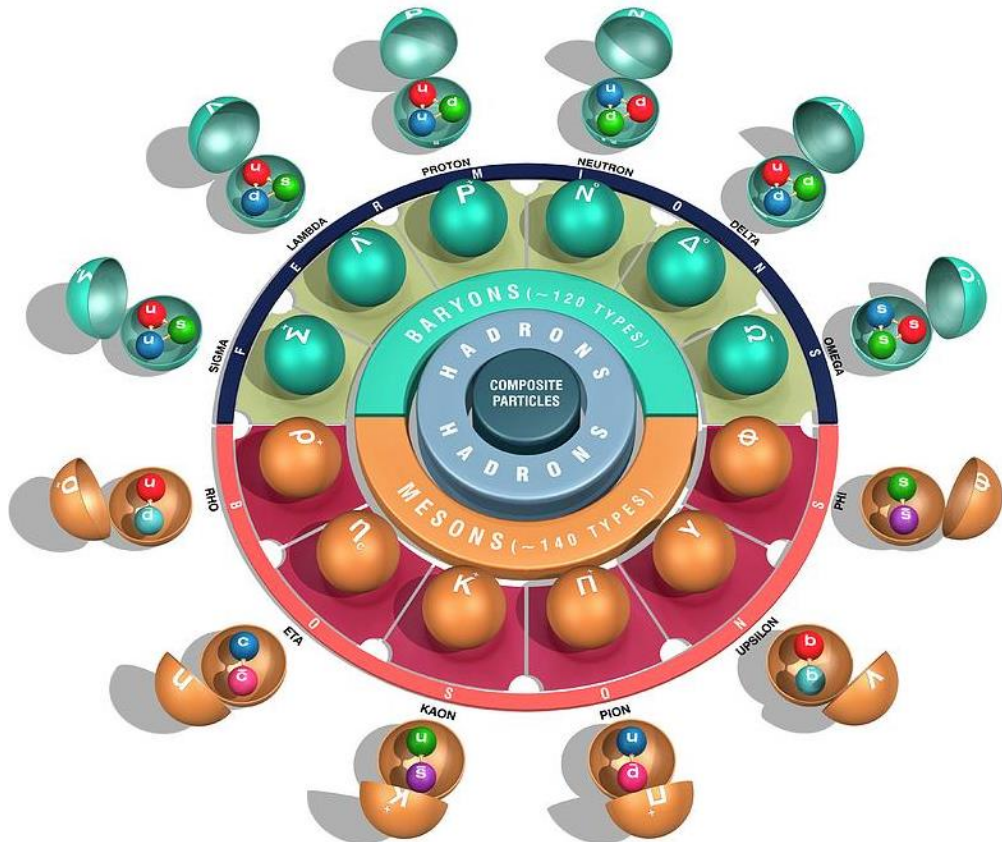
Non-perturbative
regime



Quark models

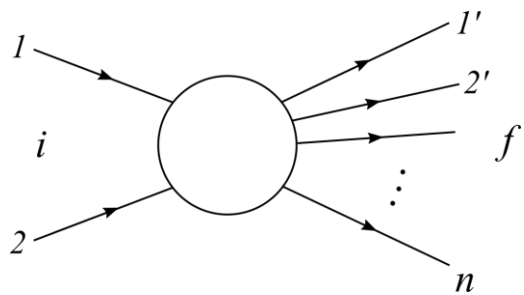
In this model the hadrons are made by constituent quarks.

Constituent quark models
does not explain
completely the hadron
structure, but are very
useful as a first tool.

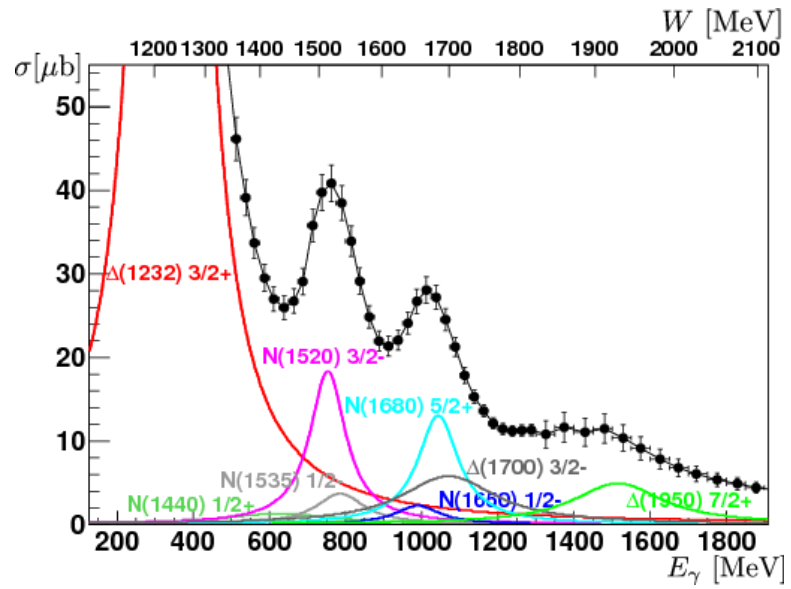


Scattering experiments

Scattering experiments are very important to study matter and its interactions



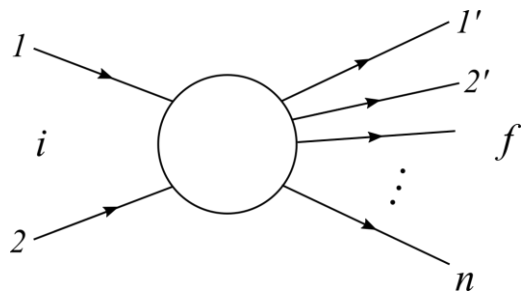
During the collision the particles can form “resonant states”, each one with well defined angular momentum.



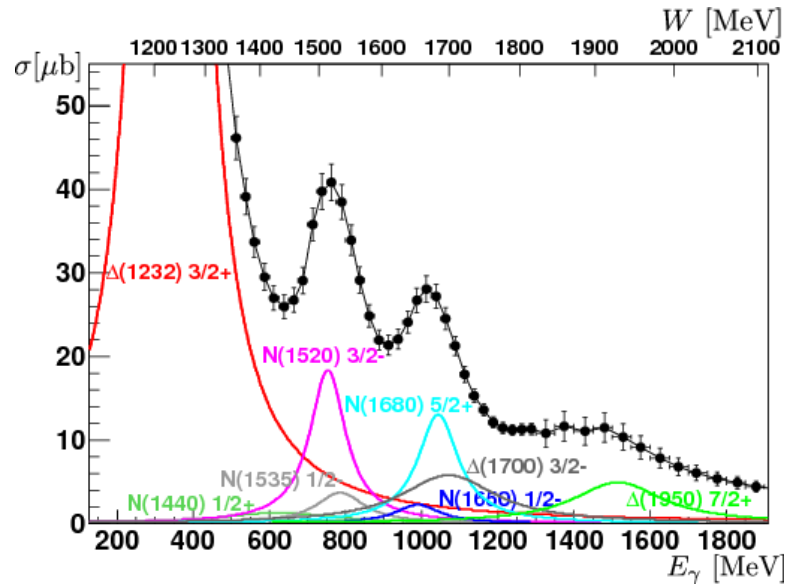
π_0 photoproduction off the proton
Thiel, A. et al. Eur.Phys.J. A53 no.1, 8 (2017)

Scattering experiments

Scattering experiments are very important to study matter and its interactions



During the collision the particles can form “resonant states”, each one with well defined angular momentum.



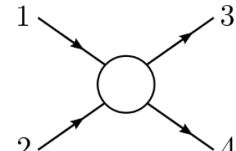
π_0 photoproduction off the proton
Thiel, A. et al. Eur.Phys.J. A53 no.1, 8 (2017)

Partial wave analysis needed to disentangle the resonances and discern the existence of states

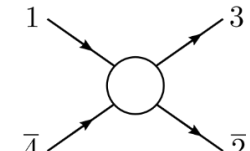
S-matrix theory

Operator whose elements quantify the transition between an initial $|a\rangle$ to a final $|b\rangle$ state.

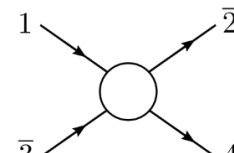
$$S(s, t) = I + 2iT(s, t)$$



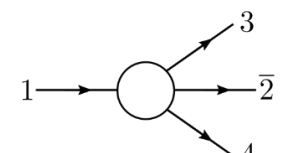
s-channel



u-channel



t-channel



decay channel

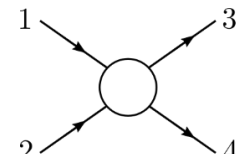
S-matrix theory

Operator whose elements quantify the transition between an initial $|a\rangle$ to a final $|b\rangle$ state.

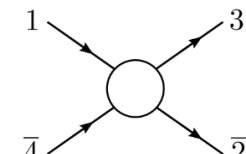
$$S(s, t) = I + 2iT(s, t)$$

- *Something happens* Unitarity
- *Causality* Analyticity
- *Particle-Antiparticle* Crossing symmetry

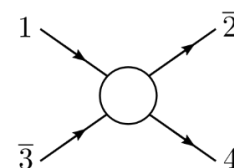
+Additional symmetries v.g. gauge, quiral, ...



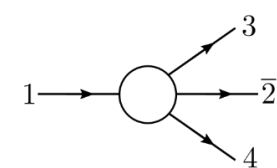
s-channel



u-channel



t-channel



decay channel

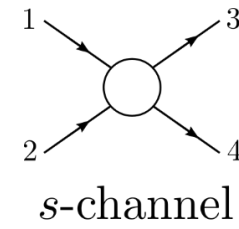
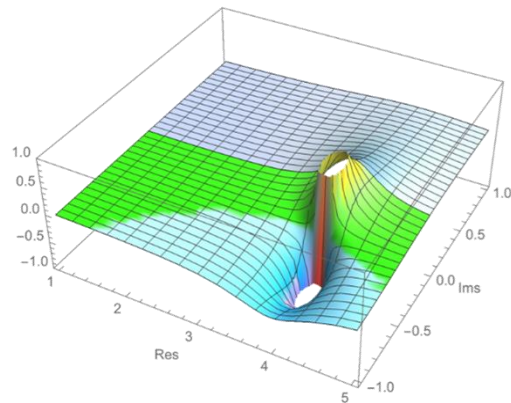
S-matrix theory

Operator whose elements quantify the transition between an initial $|a\rangle$ to a final $|b\rangle$ state.

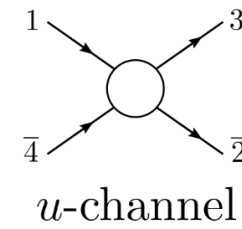
$$S(s, t) = I + 2iT(s, t)$$

- *Something happens* Unitarity
- *Causality* Analyticity
- *Particle-Antiparticle* Crossing symmetry

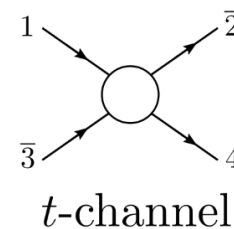
+Additional symmetries v.g. gauge, quiral, ...



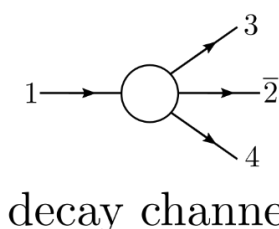
s-channel



u-channel



t-channel



decay channel

The scattering amplitude is an analytic function in the complex energy plane and is fully described by its singularities, poles and cuts.

Resonances and partial wave analysis

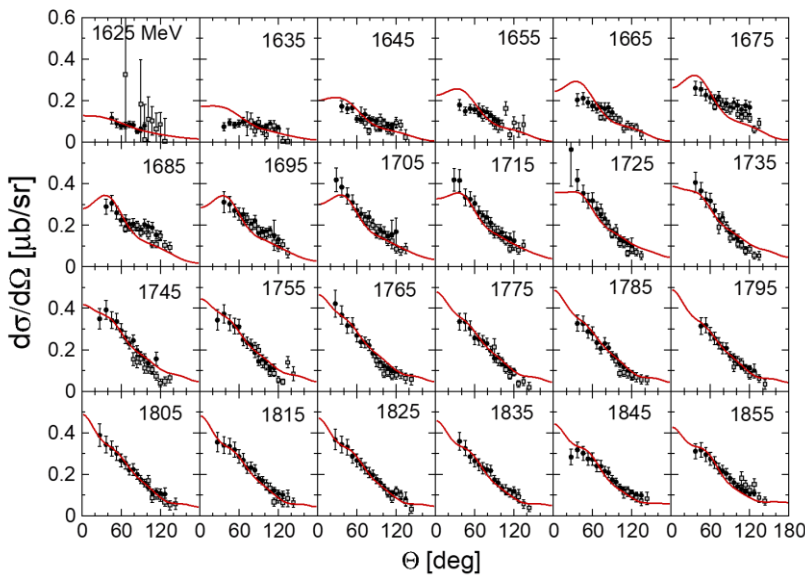
Writing the scattering amplitude in partial waves its convenient since:

- We can make contact with the angular momentum variable.
- At low energy we expect the contribution of only few partial waves.
- Each partial wave satisfies its own unitarity condition.

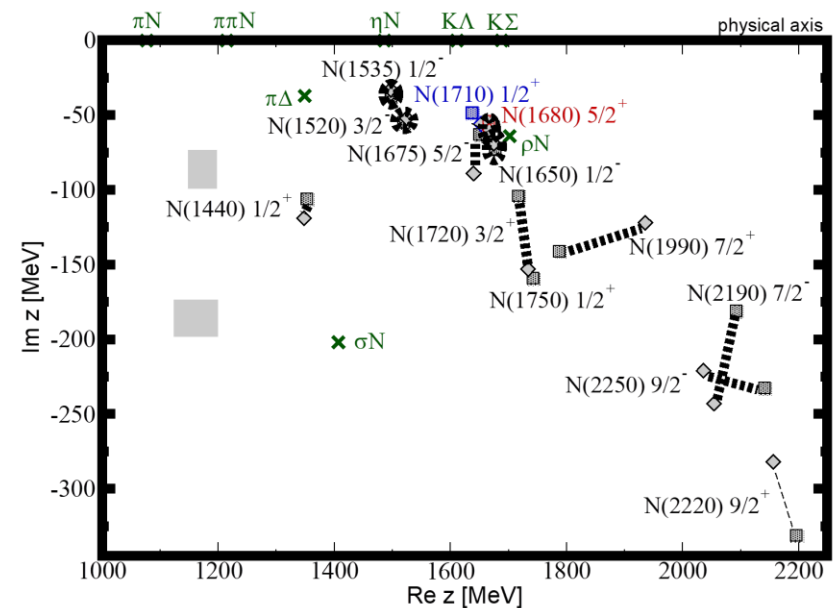
Resonances and partial wave analysis

Writing the scattering amplitude in partial waves its convenient since:

- We can make contact with the angular momentum variable.
- At low energy we expect the contribution of only few partial waves.
- Each partial wave satisfies its own unitarity condition.



Differential cross sections of the reaction $\gamma p \rightarrow K^+ \Lambda$
Rönchen, D., Döring, M. & Meißenner, U.G. Eur. Phys. J. A 54: 110 (2018).



Coupled-channel dynamics in the reactions $\pi N \rightarrow \pi N$, ηN , $K\Lambda$, $K\Sigma$
Ronchen, D. et al. Eur.Phys.J. A49 44 (2013).

Regge theory

It's based on the analytical continuation of the angular momentum

$$A(s, t) = \sum_{\ell=0}^{\infty} (2\ell + 1) f_\ell(s) P_\ell(z)$$

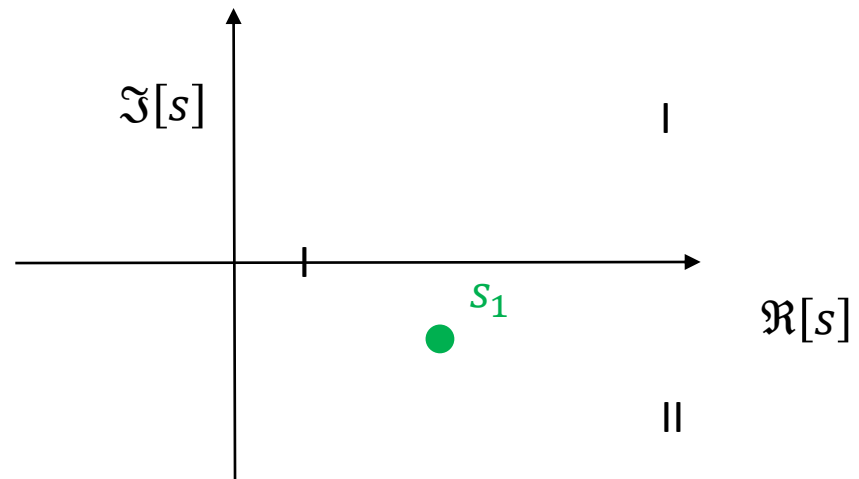
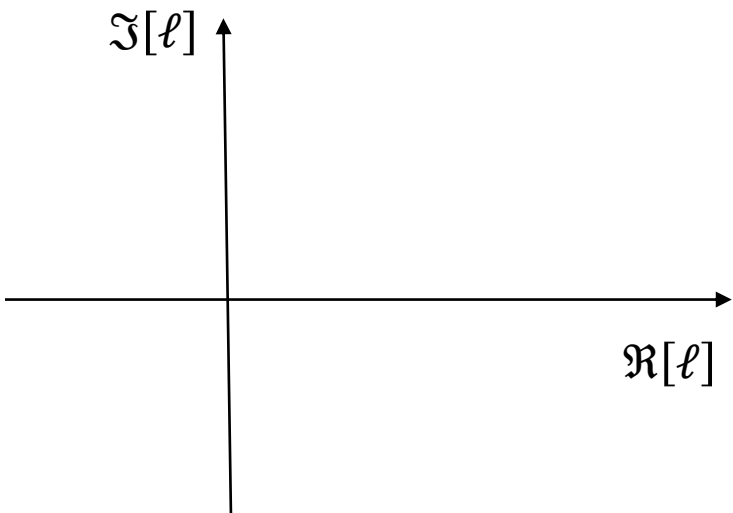
Regge theory

It's based on the analytical continuation of the angular momentum

$$A(s, t) = \sum_{\ell=0}^{\infty} (2\ell + 1) f_{\ell}(s) P_{\ell}(z)$$

\downarrow

$$f(\ell, s) \longrightarrow \ell = \ell_j$$

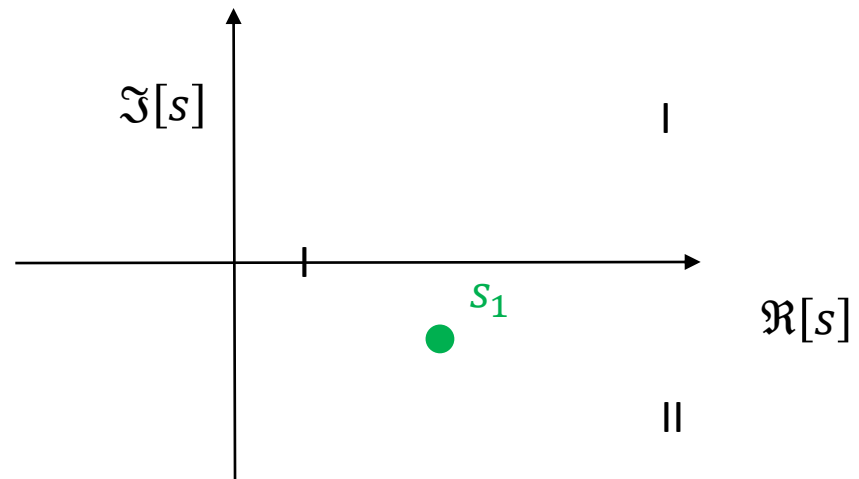
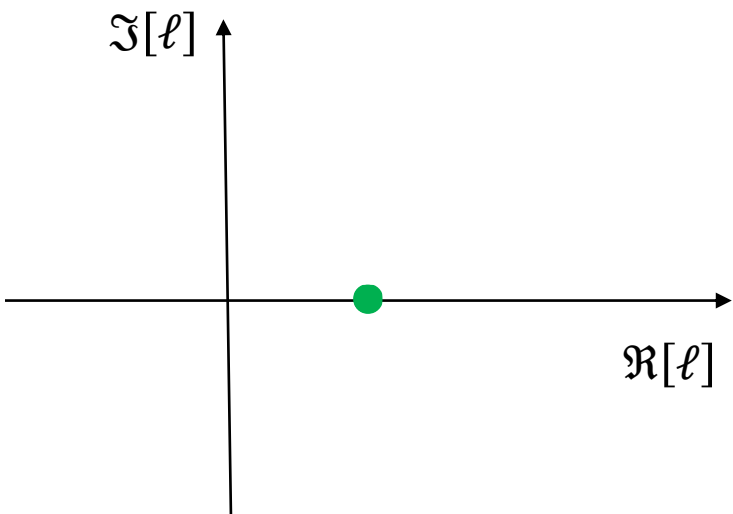


Regge theory

It's based on the analytical continuation of the angular momentum

$$A(s, t) = \sum_{\ell=0}^{\infty} (2\ell + 1) f_{\ell}(s) P_{\ell}(z)$$

$s = s_k \quad \xleftarrow{ } \quad f(\ell, s) \quad \xrightarrow{ } \quad \ell = \ell_j$

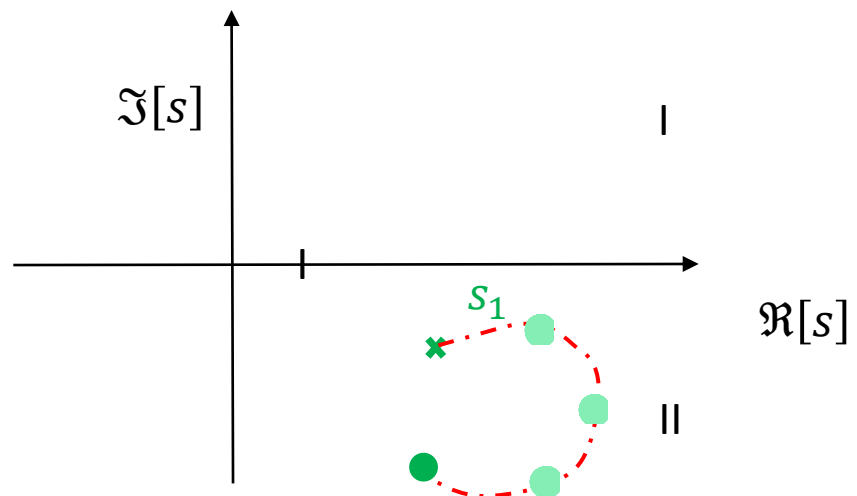
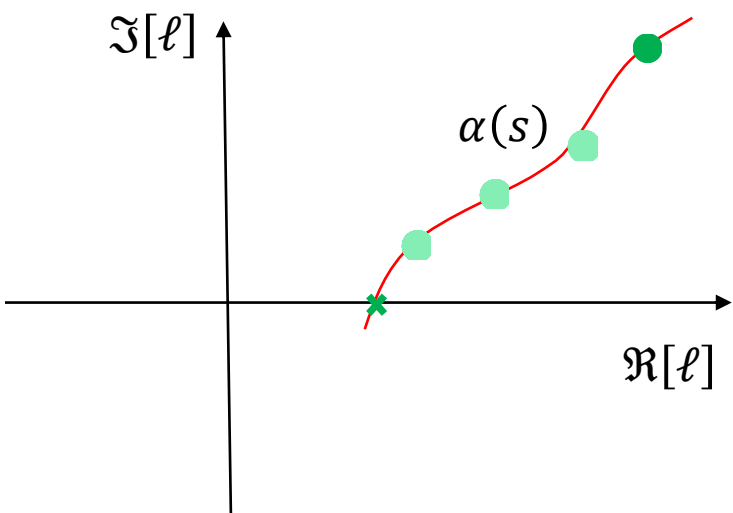


Regge theory

It's based on the analytical continuation of the angular momentum

$$A(s, t) = \sum_{\ell=0}^{\infty} (2\ell + 1) f_{\ell}(s) P_{\ell}(z)$$

$s = s_k$ $\xleftarrow{f(\ell, s)}$ $\ell = \ell_j$

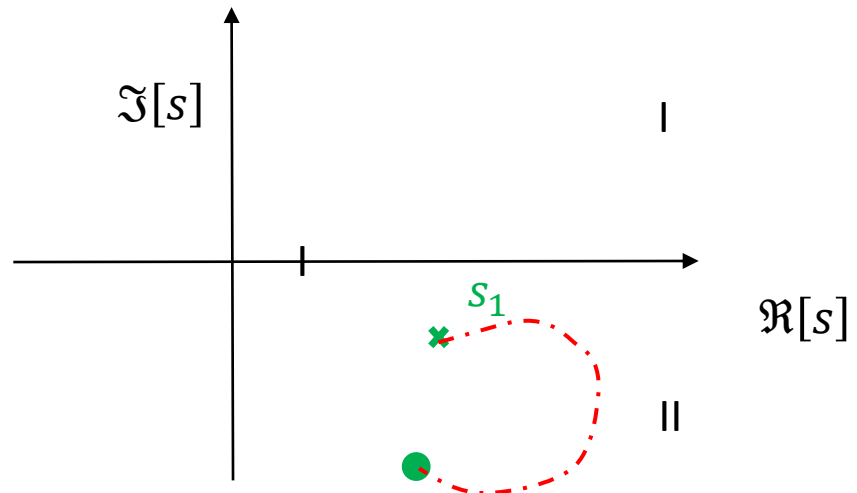
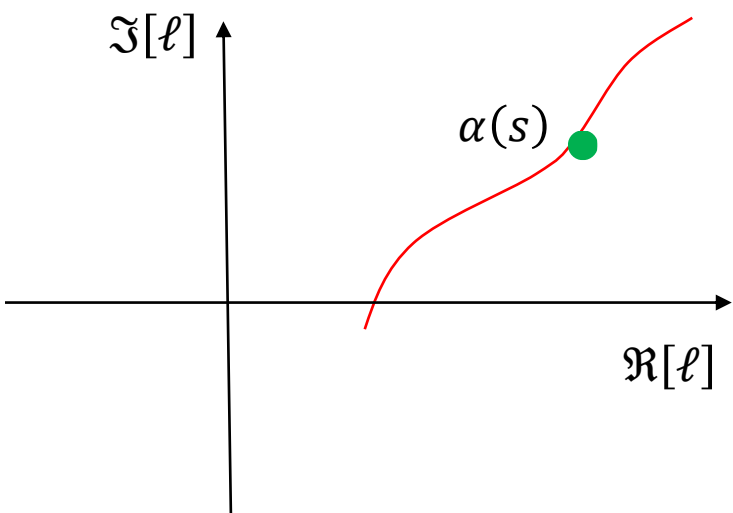


Regge theory

It's based on the analytical continuation of the angular momentum

$$A(s, t) = \sum_{\ell=0}^{\infty} (2\ell + 1) f_{\ell}(s) P_{\ell}(z)$$

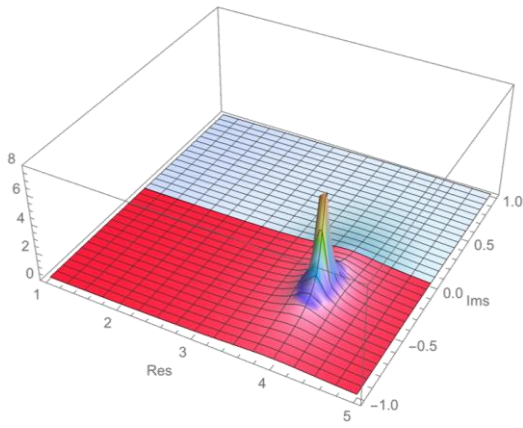
$s = s_k$ $\xleftarrow{f(\ell, s)}$ $\ell = \ell_j$



Exists a complex function called “Regge trajectory” which connects the poles of bound states and resonances.

The analytical continuation in angular momentum predicts a split of states by signature.

Regge theory in hadron spectroscopy



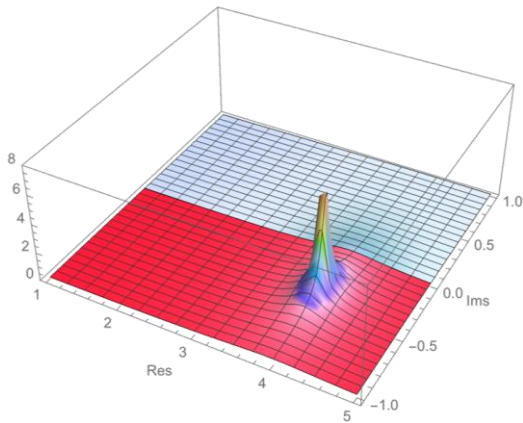
Near a pole:

$$t_\ell(s) \sim \frac{1}{M^2 - s - ig^2\rho(s, s_t)}$$

Near Regge pole:

$$t_\ell(s) \sim \frac{1}{\ell - \alpha(s)}$$

Regge theory in hadron spectroscopy



Near a pole:

$$t_\ell(s) \sim \frac{1}{M^2 - s - ig^2\rho(s, s_t)}$$

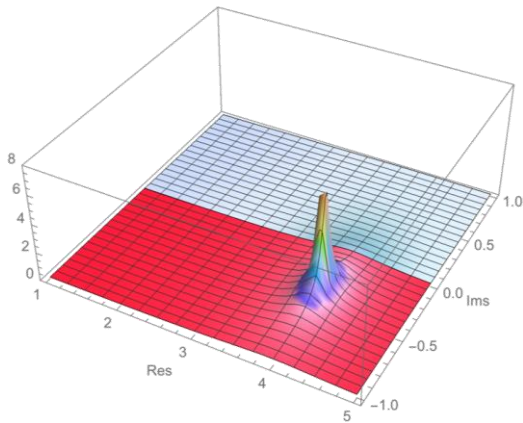
Near Regge pole:

$$t_\ell(s) \sim \frac{1}{\ell - \alpha(s)}$$

Parametrization

$$\alpha(s) = \alpha_0 + \alpha's + i\gamma\phi(s, s_t)$$

Regge theory in hadron spectroscopy



Near a pole:

$$t_\ell(s) \sim \frac{1}{M^2 - s - ig^2\rho(s, s_t)}$$

Near Regge pole:

$$t_\ell(s) \sim \frac{1}{\ell - \alpha(s)}$$

Parametrization

$$\alpha(s) = \alpha_0 + \alpha's + i\gamma\phi(s, s_t)$$

- Hadronic spectrum has a near linear Regge trajectory.
- Linear trajectories are a phenomenological indication of confinement.
- States belonging to linear trajectories are expected to be closely connected to quark model predictions.
- The “slope” parameter is related with high energy analysis.

N^* and Δ^* pole extractions

There are many models for the analysis based on S-matrix principles, but they do not consider the restrictions that Regge theory imposes.

We select pole extractions from πN scattering which also provides errors

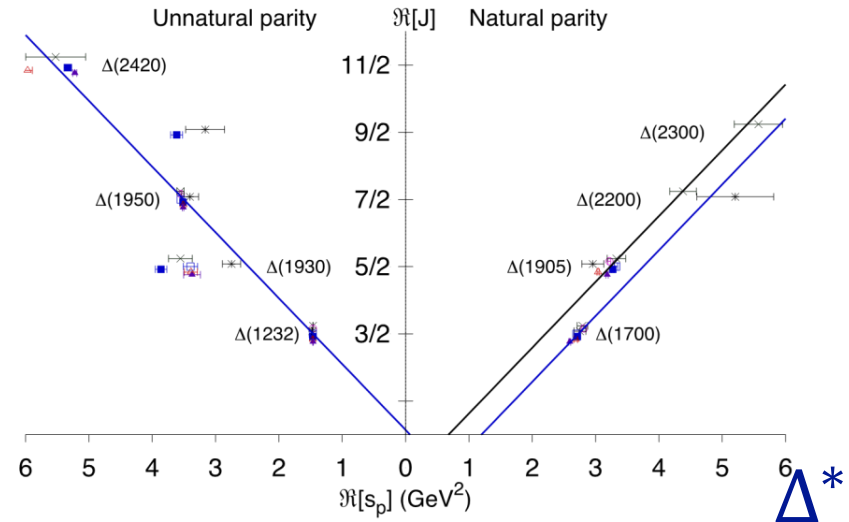
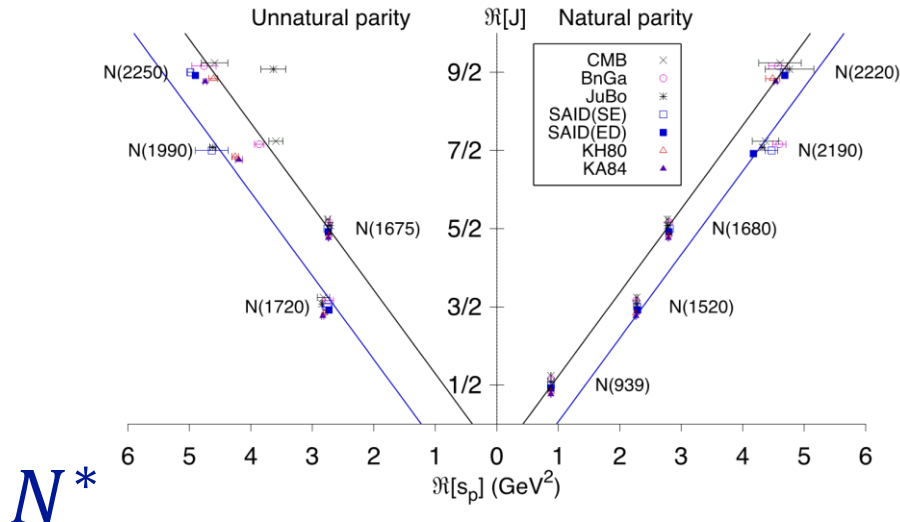
N^* and Δ^* pole extractions

There are many models for the analysis based on S-matrix principles, but they do not consider the restrictions that Regge theory imposes.

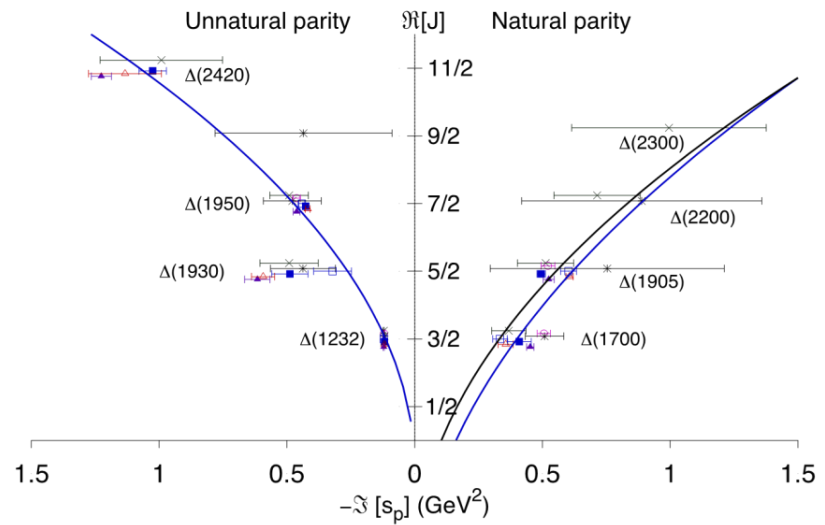
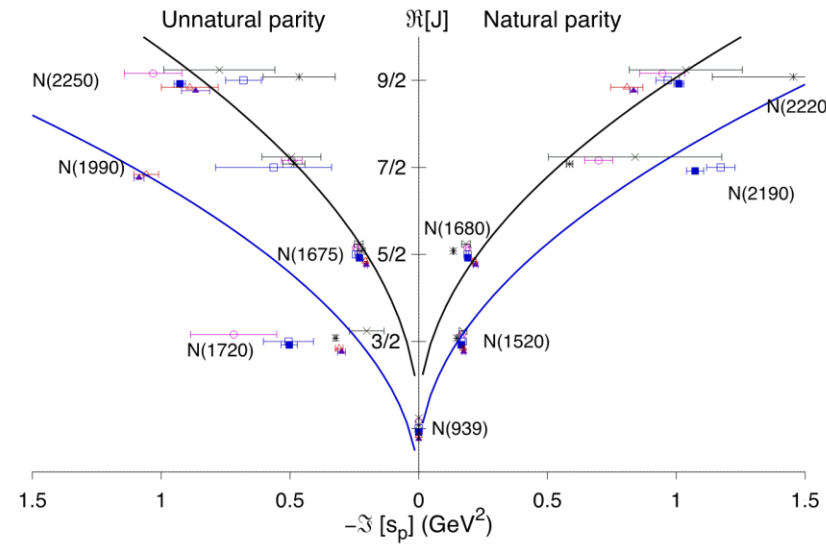
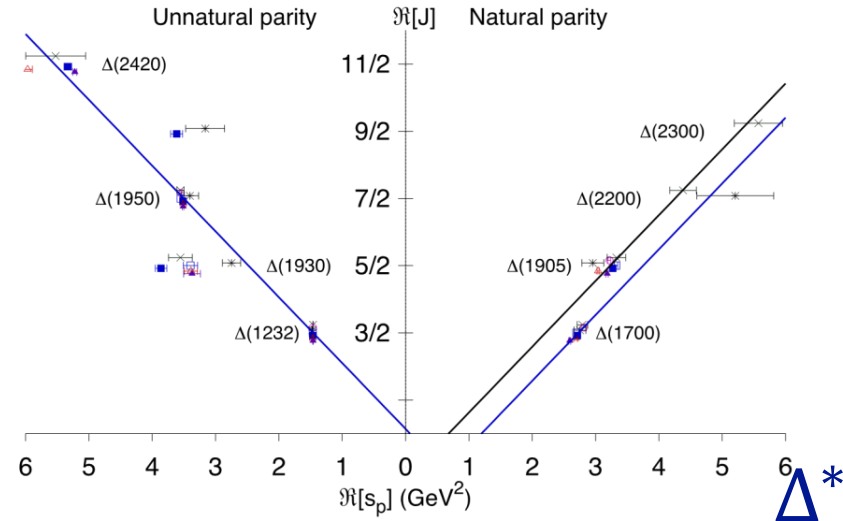
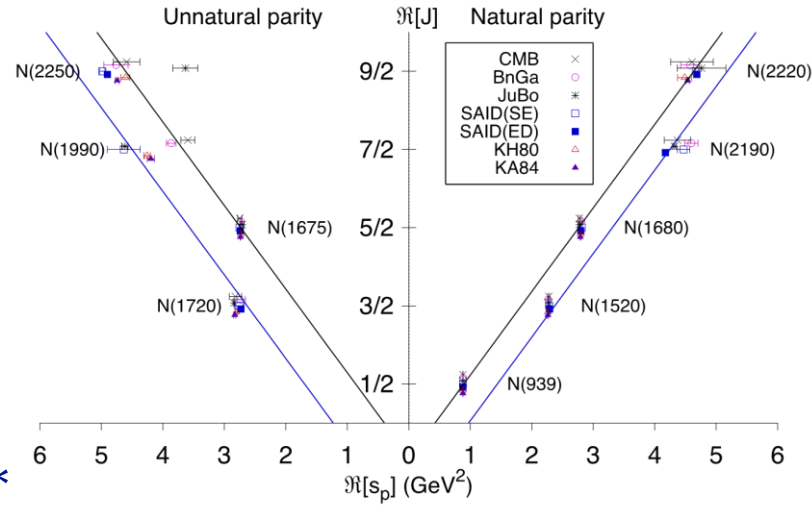
We select pole extractions from πN scattering which also provides errors

- **CMB**: Carnegie-Mellon-Berkeley partial wave analysis.
- **JüBo**: Jülich-Bonn coupled channel model.
- **BnGa**: Bonn-Gatchina multichannel partial wave analysis.
- **SAID(SE)**: SAID-GW WI08 single energy partial wave analysis using the Laurent+Pietarinen (LP) approach.
- **SAID(ED)**: SAID-GW WI08 energy dependent partial wave analysis using the LP approach.
- **KH80**: Partial wave analysis Karlsruhe-Helsinki KH80 using LP.
- **KA84**: Partial wave analysis Karlsruhe-Helsinki KH84 using LP.

Chew-Frautschi plots

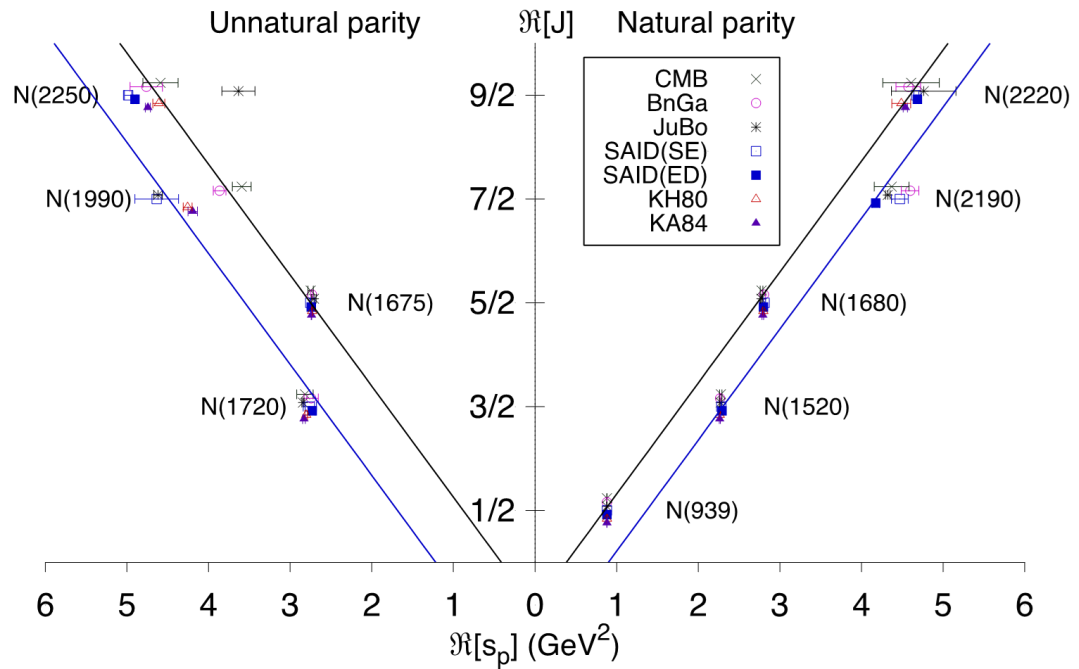


Chew-Frautschi and $(\Im[s_p], \Re[J] = J_P)$ plots



Classification of the Regge trajectories

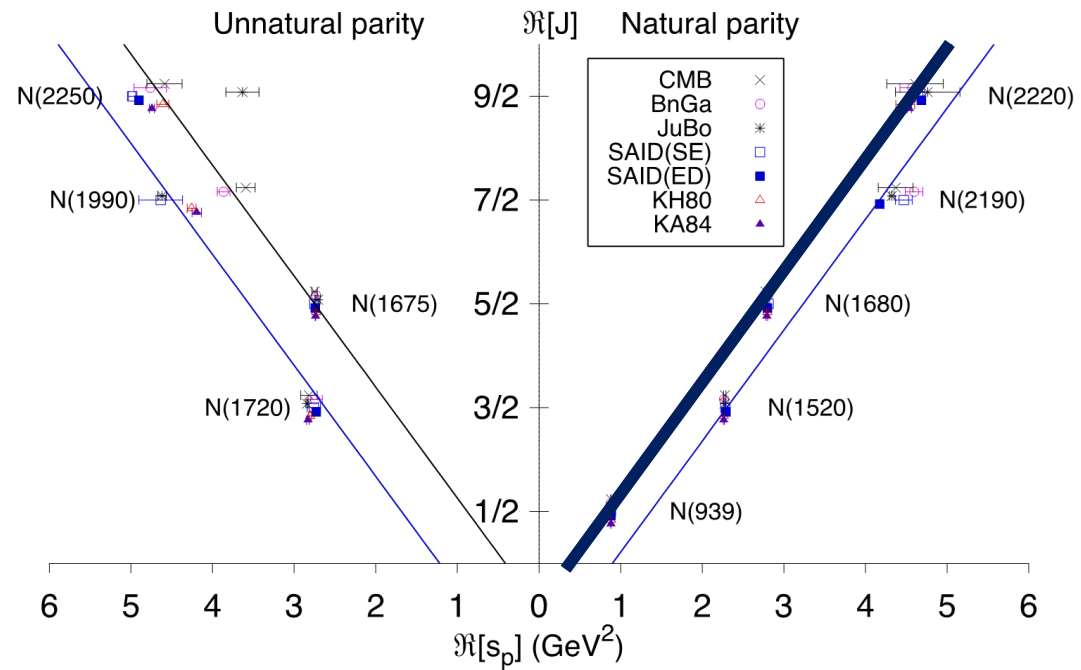
Let I the isospin, η the naturality, J_P the spin, P parity and τ signature, we classify the states in the trajectories as $I_{(\tau)}^\eta$



$$\eta = \tau P. \text{ For baryons } \eta = +1 \text{ si } P = (-1)^{J_P - \frac{1}{2}}$$
$$\eta = -1 \text{ si } P = -(-1)^{J_P - \frac{1}{2}}$$

Classification of the Regge trajectories

Let I the isospin, η the naturality, J_P the spin, P parity and τ signature, we classify the states in the trajectories as $I_{(\tau)}^\eta$

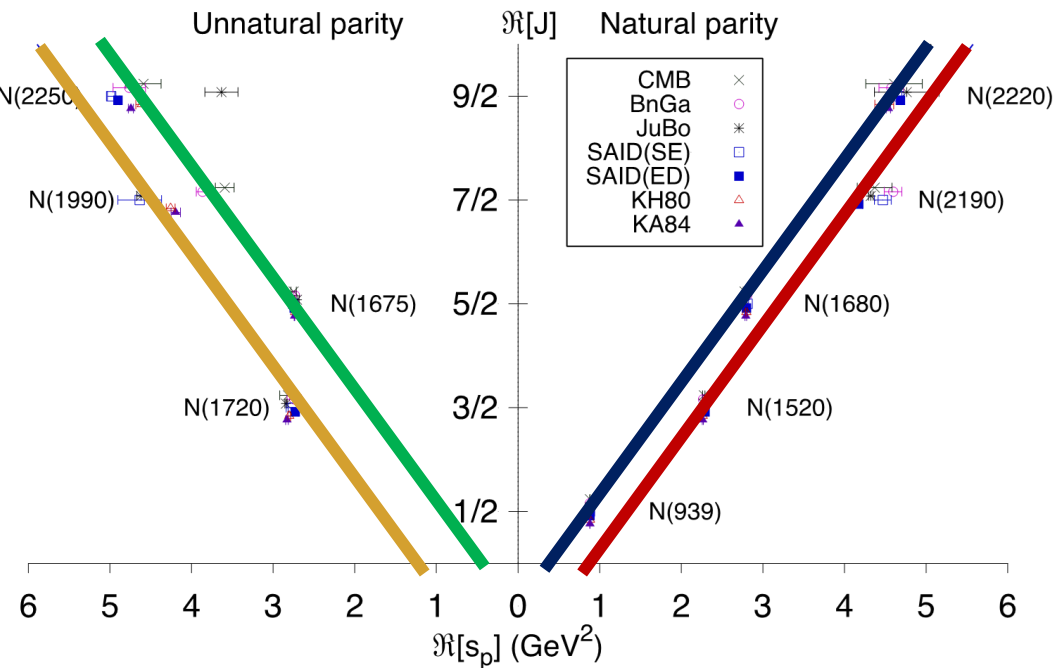
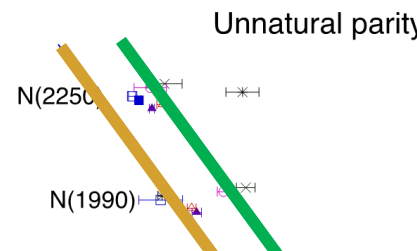
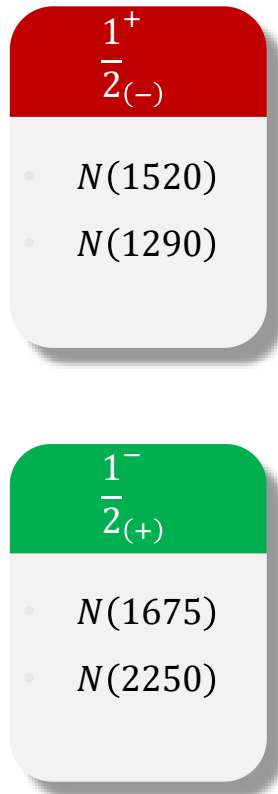
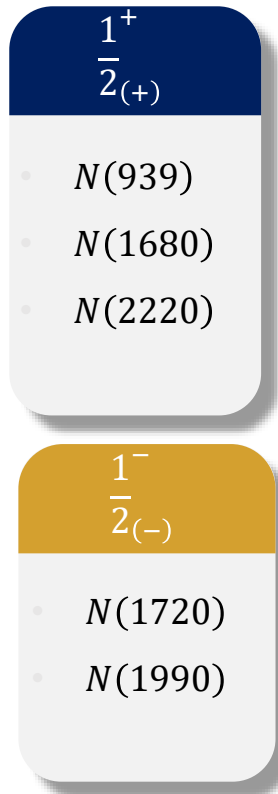


$$\eta = \tau P. \text{ For baryons } \eta = +1 \text{ si } P = (-1)^{J_P - \frac{1}{2}}$$

$$\eta = -1 \text{ si } P = -(-1)^{J_P - \frac{1}{2}}$$

Classification of the Regge trajectories

Let I the isospin, η the naturality, J_P the spin, P parity and τ signature, we classify the states in the trajectories as $I_{(\tau)}^\eta$

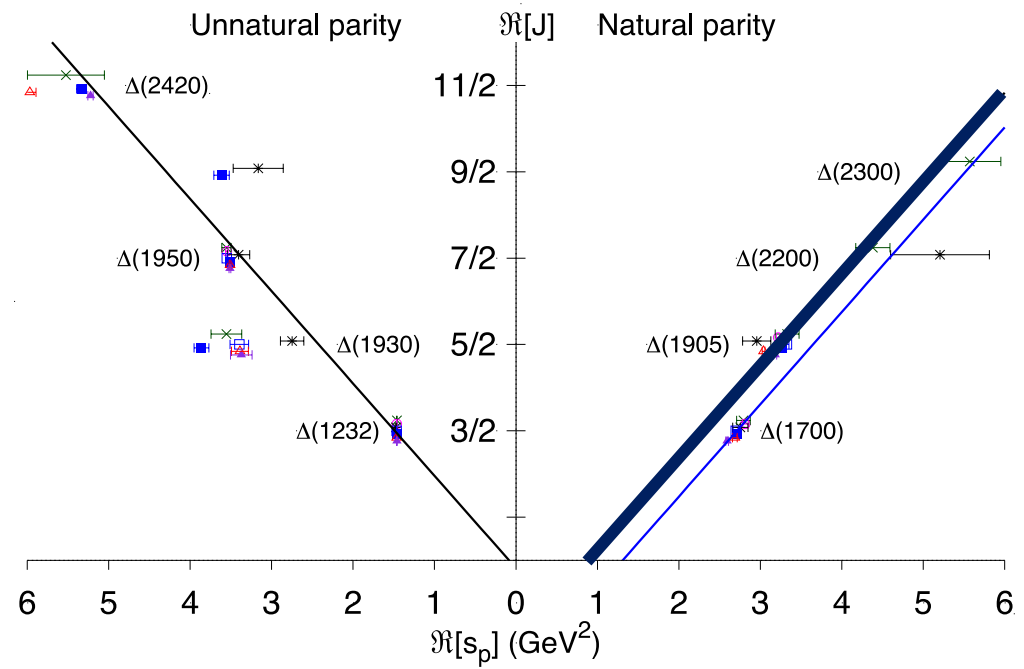
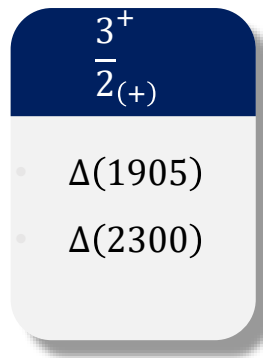


$$\eta = \tau P. \text{ For baryons } \eta = +1 \text{ si } P = (-1)^{J_P - \frac{1}{2}}$$

$$\eta = -1 \text{ si } P = -(-1)^{J_P - \frac{1}{2}}$$

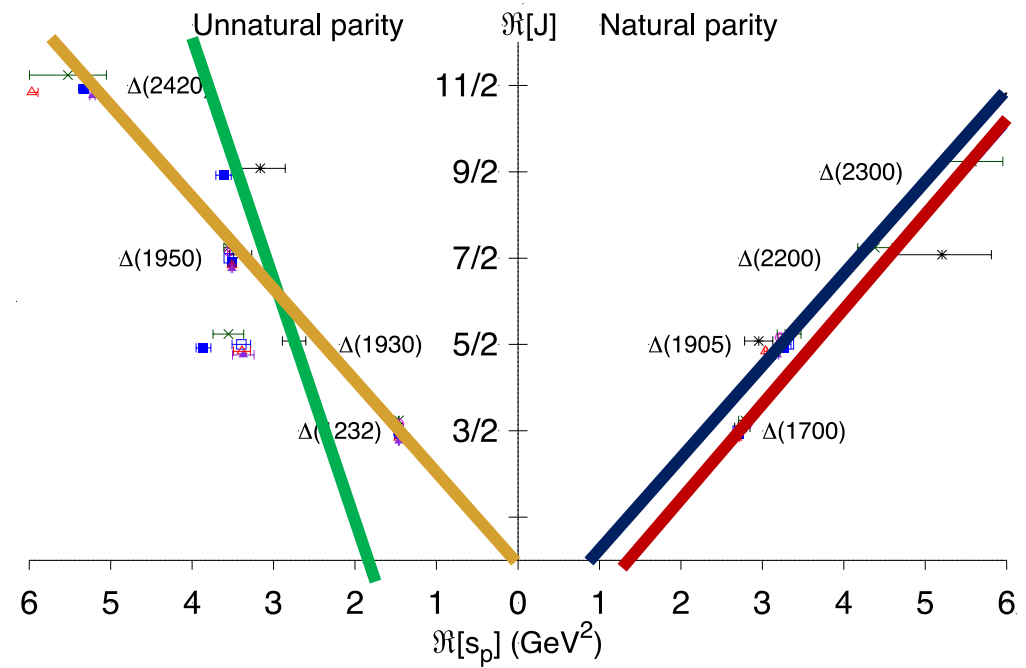
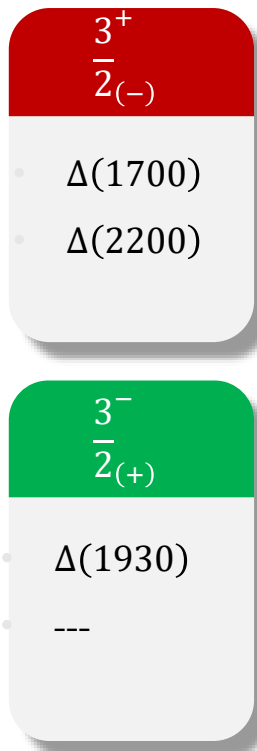
Classification of the Regge trajectories

Let I the isospin, η the naturality, J_P the spin, P parity and τ signature, we classify the states in the trajectories as $I_{(\tau)}^\eta$



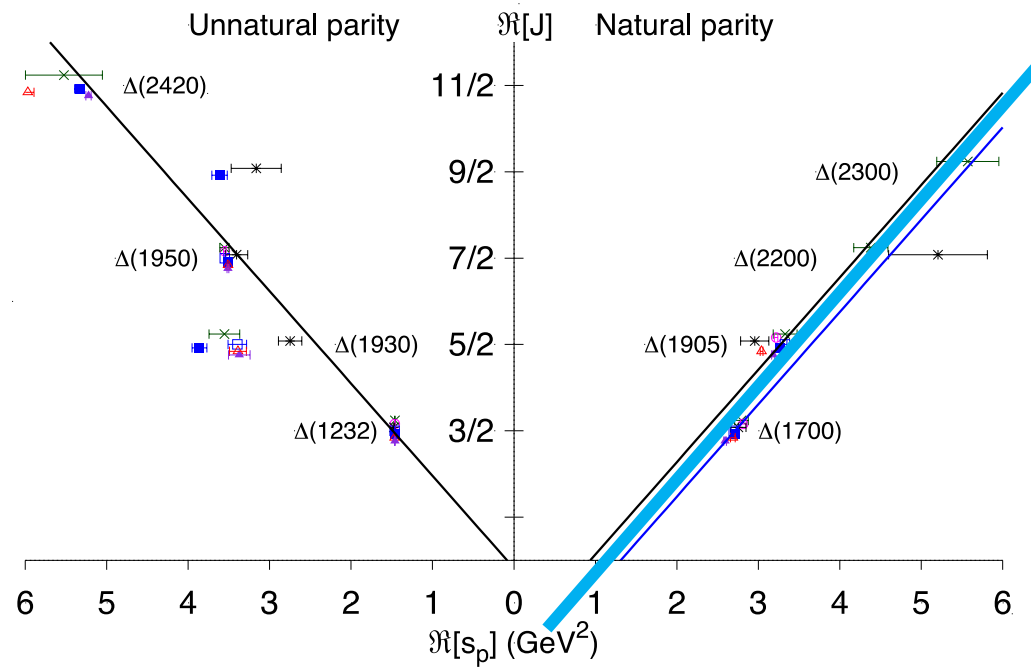
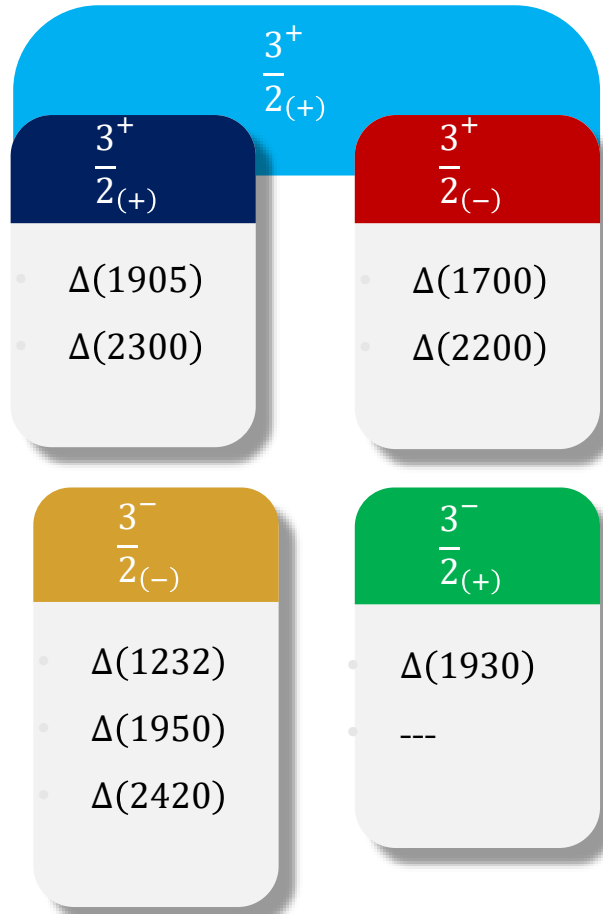
Classification of the Regge trajectories

Let I the isospin, η the naturality, J_P the spin, P parity and τ signature, we classify the states in the trajectories as $I_{(\tau)}^\eta$



Classification of the Regge trajectories

Let I the isospin, η the naturality, J_P the spin, P parity and τ signature, we classify the states in the trajectories as $I_{(\tau)}^\eta$



Model description

Hypothesis.– The square-root-like behavior is the leading singularity of the trajectories as implied by unitarity and is mainly due to the contribution of the phase space to the dispersion amplitude.

- **Model 0** $i\phi_0(s, s_t) = 0$
- **Model I** $i\phi_I(s, s_t) = i\sqrt{s - s_t}$
- **Model II** $i\phi_{II}(s, s_t) = \frac{2}{i\pi} \frac{s - s_t}{\sqrt{s(s_t - s)}} \arctan \sqrt{\frac{s}{s_t - s}} + 2i \sqrt{1 - \frac{s_t}{s}}$ (Dispersive)

Model description

Hypothesis.– The square-root-like behavior is the leading singularity of the trajectories as implied by unitarity and is mainly due to the contribution of the phase space to the dispersion amplitude.

- **Model 0** $i\phi_0(s, s_t) = 0$
- **Model I** $i\phi_I(s, s_t) = i\sqrt{s - s_t}$
- **Model II** $i\phi_{II}(s, s_t) = \frac{2}{i\pi} \frac{s - s_t}{\sqrt{s(s_t - s)}} \arctan \sqrt{\frac{s}{s_t - s}} + 2i \sqrt{1 - \frac{s_t}{s}}$ (Dispersive)

On average the description must be approximately correct because of the linear and square-root-like behaviors, but our model is incomplete, so, deviations from the models are associated to the physics that our model lacks, i.e., additional QCD dynamics, which we interpret as physics that go beyond the 3q picture.

Monte Carlo analysis

We generate pseudo-data for the pole positions for the N^* and Δ^* according to the uncertainties

We fit each sample for a given trajectory minimizing the distance:

$$d^2 = \sum_{poles} \left\{ [\Re[J] - \Re[\alpha(s_P)]]^2 + [\Im[J] - \Im[\alpha(s_P)]]^2 \right\}$$

We repeat the process 10^4 times to have enough statistics to compute the expected value and uncertainty of each parameter.

Monte Carlo analysis

We generate pseudo-data for the pole positions for the N^* and Δ^* according to the uncertainties

We fit each sample for a given trajectory minimizing the distance:

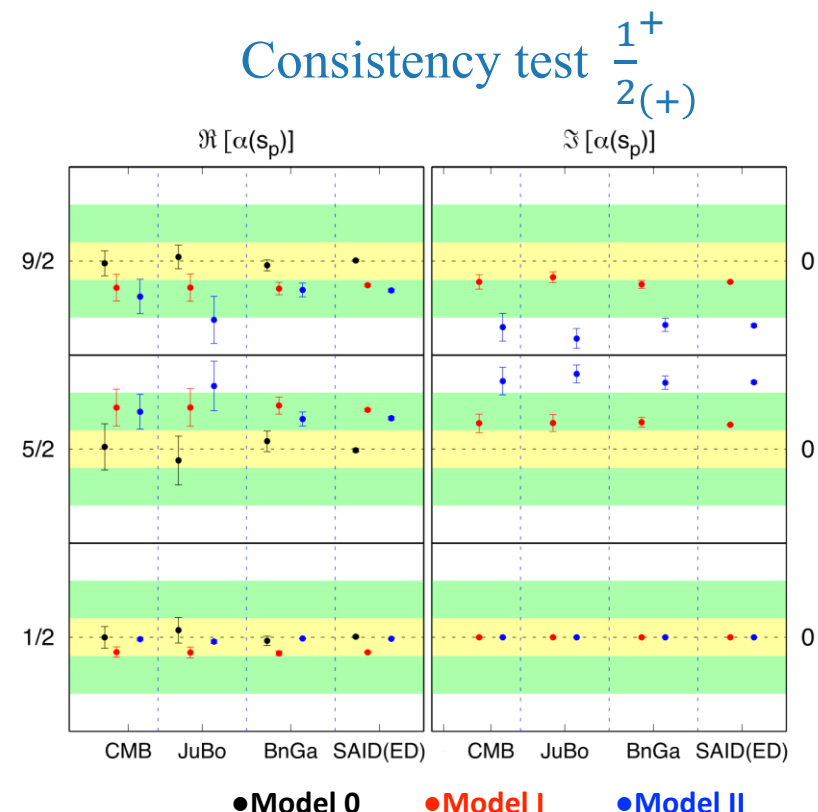
$$d^2 = \sum_{poles} \left\{ [\Re[J] - \Re[\alpha(s_P)]]^2 + [\Im[J] - \Im[\alpha(s_P)]]^2 \right\}$$

We repeat the process 10^4 times to have enough statistics to compute the expected value and uncertainty of each parameter.

In the pole position we must recover the physical angular momentum, this is our “consistency check”.

Results for the $\frac{1}{2}^+$

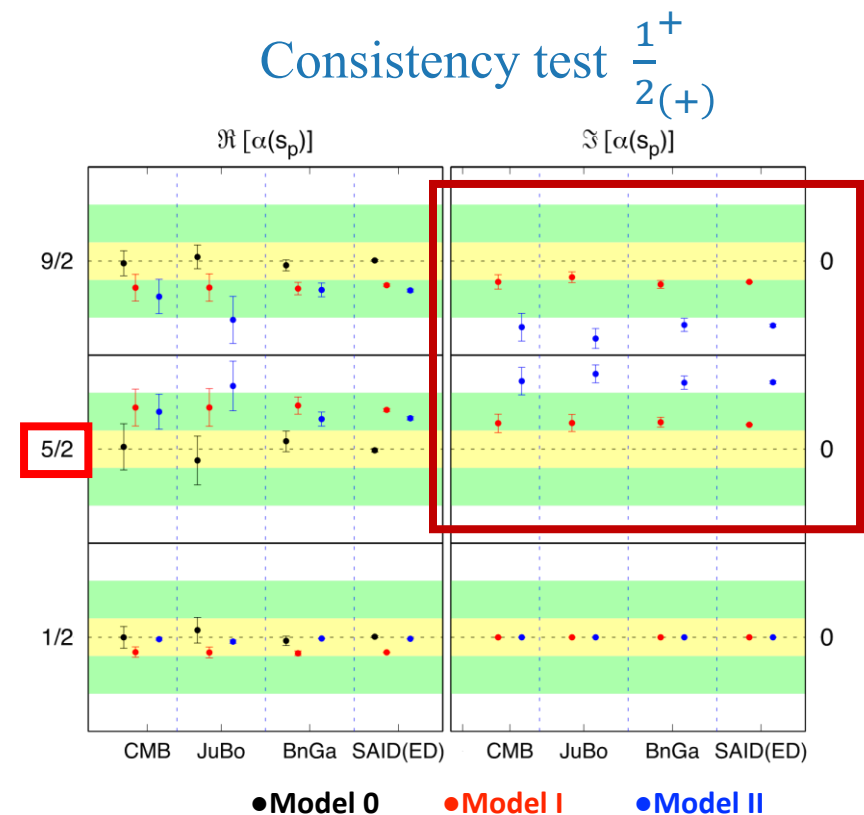
- There is tension between the models.
- $N(939)$ is better described by the disp. model
- $N(1680)$ gives a signal beyond $3q$ picture, because it has small errors.
- α' is compatible with high energy information ($\approx 0.98 \text{ GeV}^{-2}$)*.



* J. Van de Wiele and S. Ong, EPJA 46 (2010) 291

Results for the $\frac{1}{2}^+$

- There is tension between the models.
- $N(939)$ is better described by the disp. model
- $N(1680)$ gives a signal beyond $3q$ picture, because it has small errors.
- α' is compatible with high energy information ($\approx 0.98 \text{ GeV}^{-2}$)*.

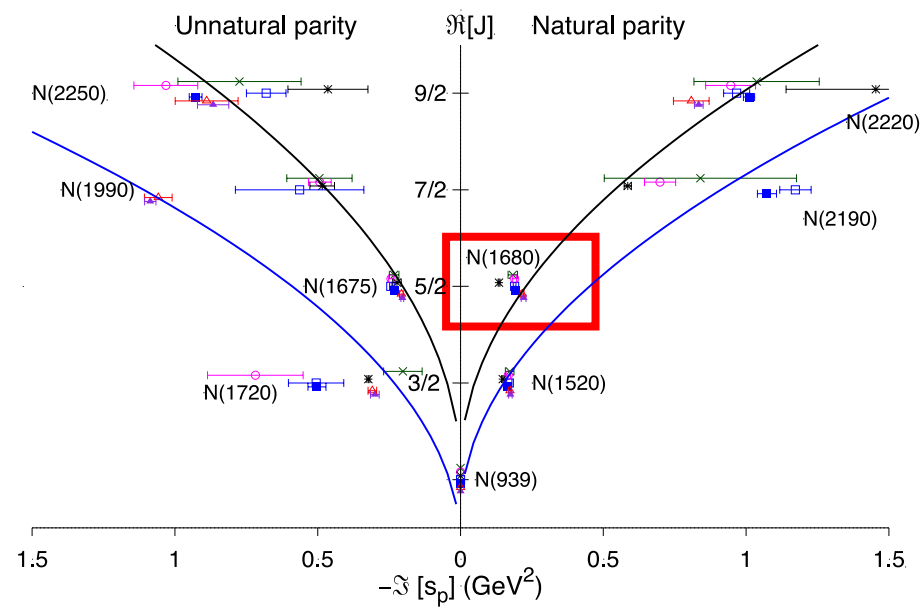
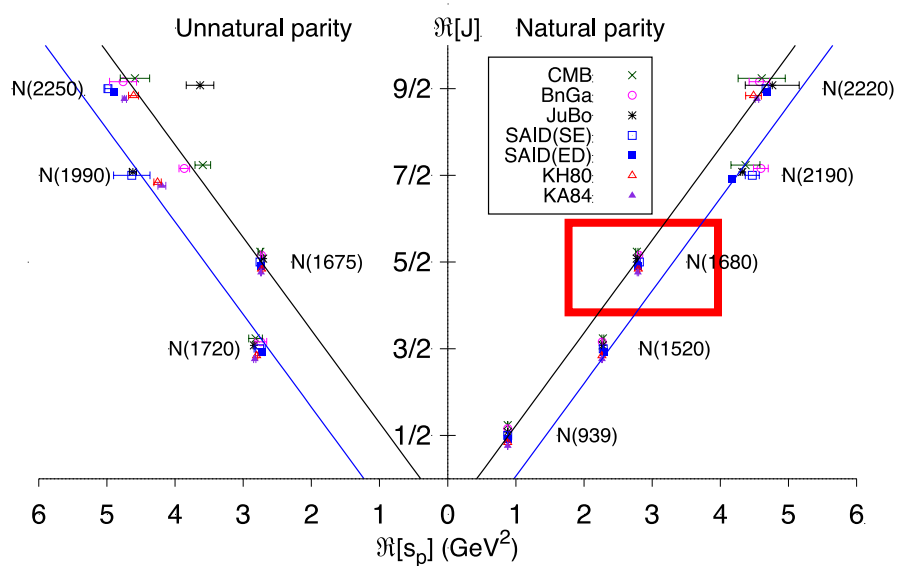


* J. Van de Wiele and S. Ong, EPJA 46 (2010) 291

$$\begin{aligned}\alpha_0 &= 0.21 \pm 0.38 \\ \gamma &= 0.651 \pm 0.040\end{aligned}$$

$$\begin{aligned}\alpha' &= 0.99 \pm 0.12 \text{ GeV}^{-2} \\ s_t &= 1.02 \pm 0.13 \text{ GeV}^{-2}\end{aligned}$$

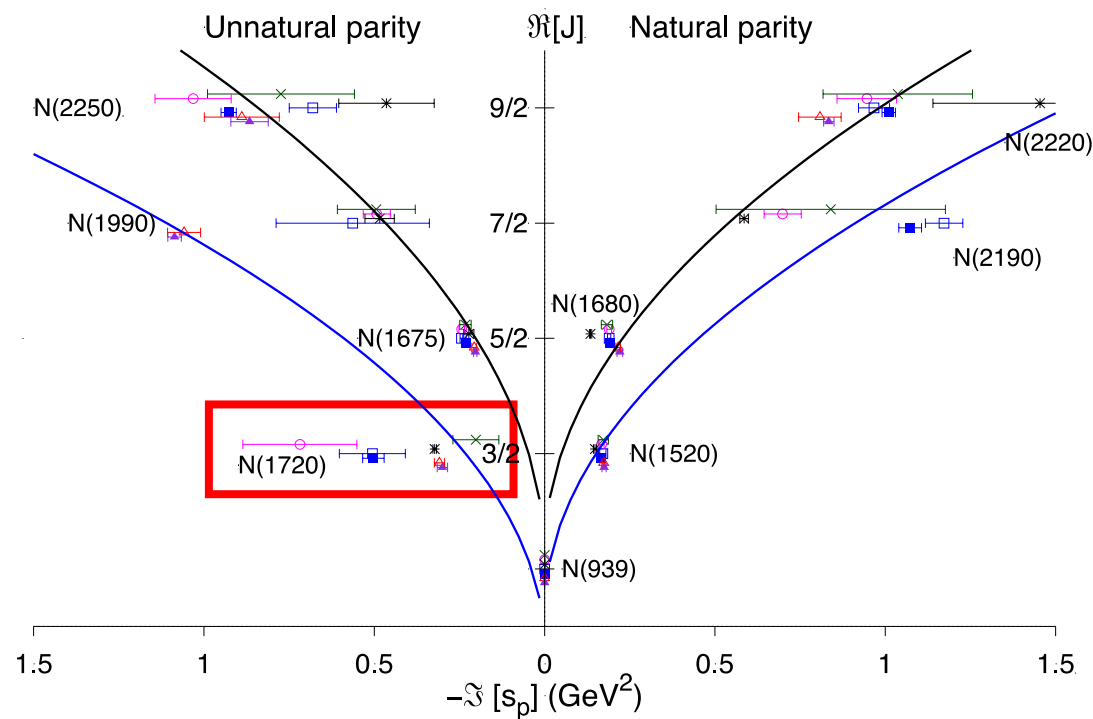
Results for the $\frac{1}{2}^+$



Results for the $\frac{1}{2}^-$

- MacDowell symmetry imposes that the slopes of $\frac{1}{2}(+)\frac{+}{-}$ and $\frac{1}{2}(-)\frac{-}{+}$ ($\frac{3}{2}(+)\frac{+}{-}$ and $\frac{3}{2}(-)\frac{-}{+}$) must be equal. It is fulfilled by SAID(SE) and BnGa approximately.
- $N(1720)$ has discrepancies among pole extractions, it is possible that the analyses are reporting not just one resonant state but an effective pole that accounts for a more complicated picture.
- $N(1720)$ is a doublet partner of the $N(1680)$, which we identified as a state with physics beyond the $3q$ picture.

Results for the $\frac{1}{2}^-$



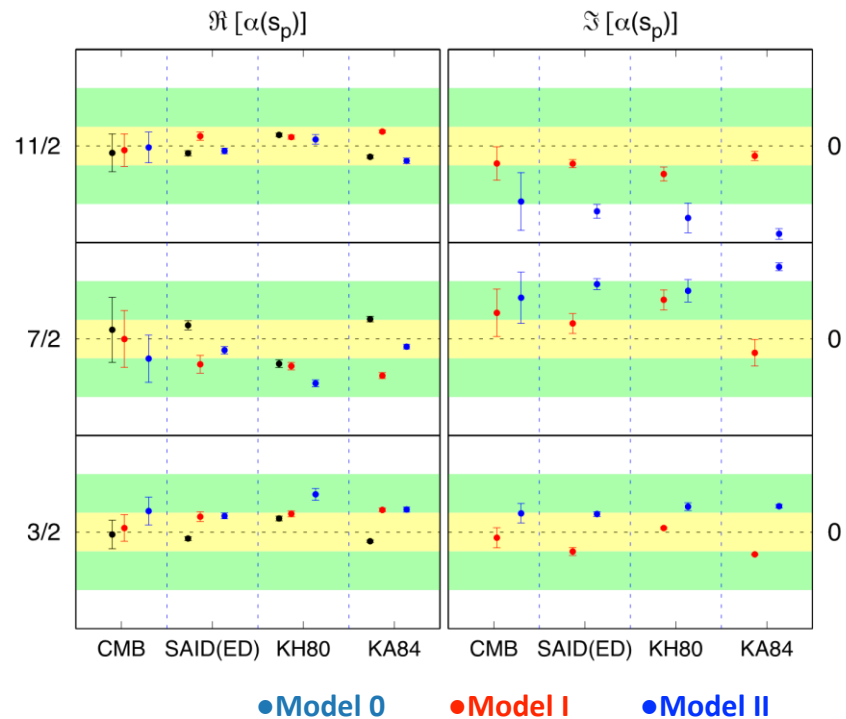
Results for the $\frac{3}{2}^+$

- This is the least known parent trajectory with large uncertainties.
- We assume degeneracy in the fits so α_0 parameter provides no information.
- **JüBo** extraction is the most consistent one, although with very large error bars.
- None of the pole sets provides a complete picture of this trajectory.

Results for the $\frac{3}{2}^-$

- $\Delta(1930)$ is not well determined by the pole extractions.
- Model II (dispersive) gives results in agreement with high energy information.
- Qualitatively the plots for $\frac{3}{2}^-_{2(-)}$ show a clear linear and square-root pattern.
- For the trajectory $\frac{3}{2}^-_{2(-)}$, poles are known well enough to be sensitive to these beyond compact 3q effects.

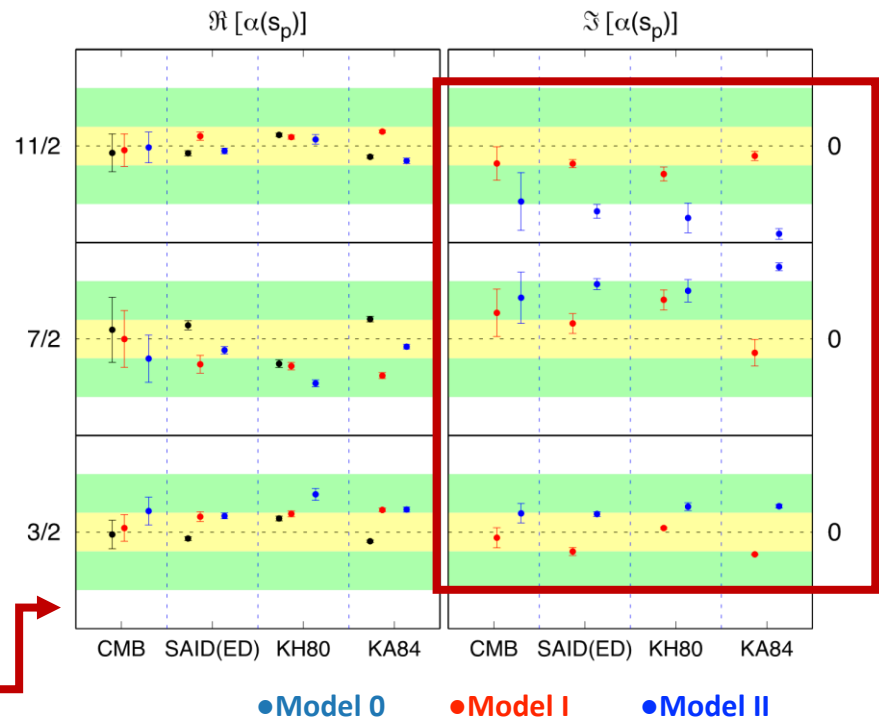
Consistency check for $\frac{3}{2}^-_{2(-)}$



Results for the $\frac{3}{2}^-$

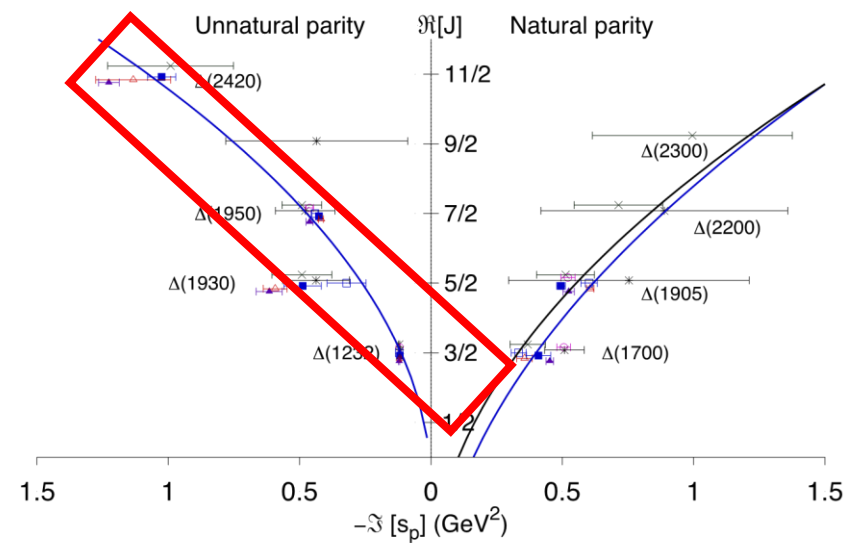
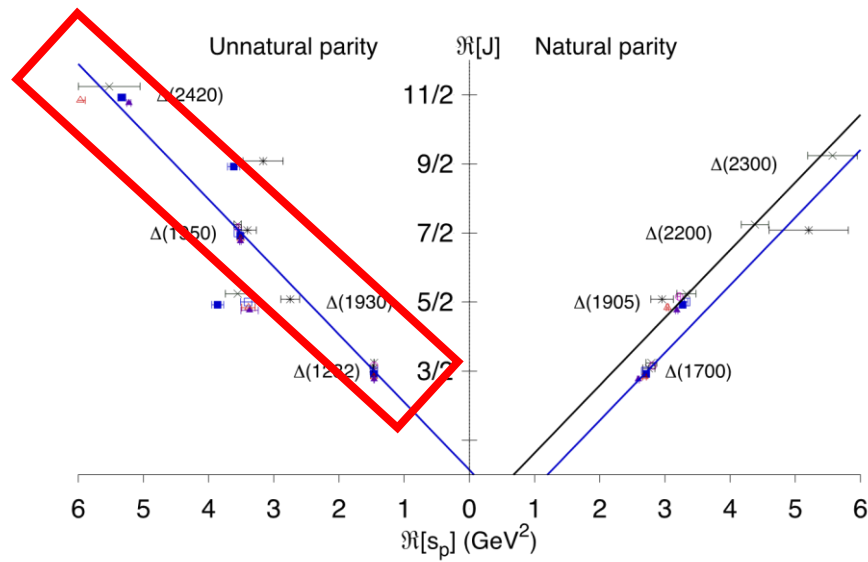
- $\Delta(1930)$ is not well determined by the pole extractions.
- Model II (dispersive) gives results in agreement with high energy information.
- Qualitatively the plots for $\frac{3}{2}^-_{2(-)}$ show a clear linear and square-root pattern.
- For the trajectory $\frac{3}{2}^-_{2(-)}$, poles are known well enough to be sensitive to these beyond compact 3q effects.

Consistency check for $\frac{3}{2}^-_{2(-)}$

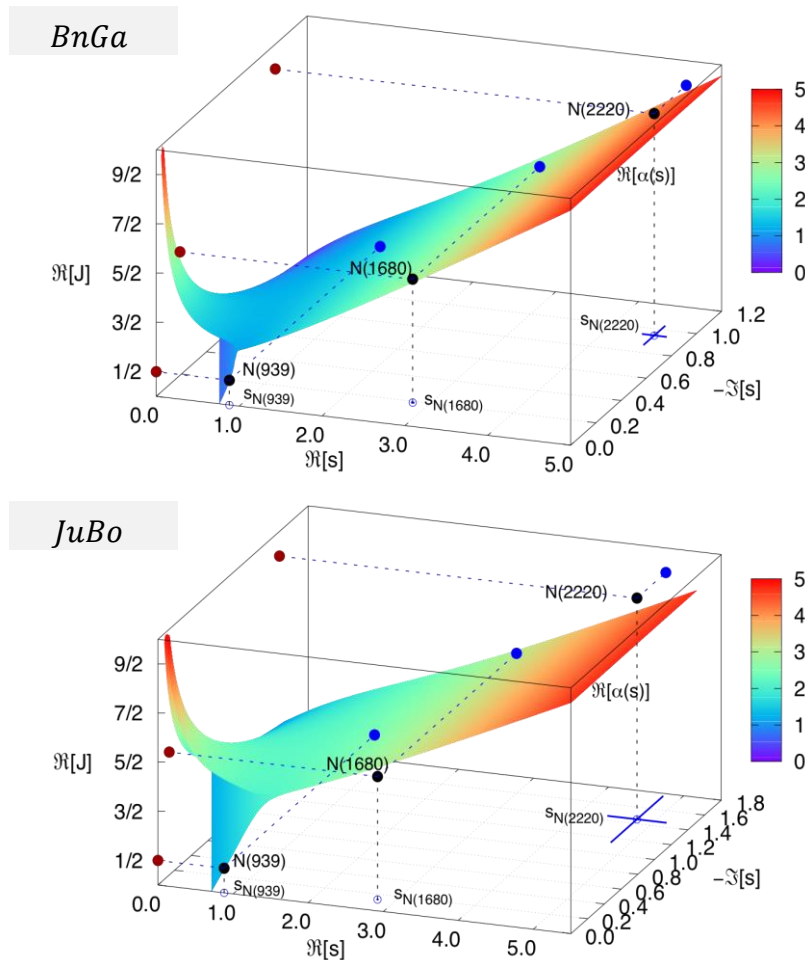


$$\begin{aligned}\alpha_0 &= -0.45 \pm 0.44 & \alpha' &= 1.21 \pm 0.15 \text{ GeV}^2 \\ \gamma &= 0.86 \pm 0.22 & s_t &= 1.52 \pm 0.12 \text{ GeV}^2\end{aligned}$$

Results for the $\frac{3}{2}^-$



Parameter space exploration



The Regge trajectory is a complex function here we show the $\Re[\alpha(s)]$ adjusted to the trajectory $\frac{1}{2}^+$ for the pole extractions of BnGa and JüBo for the model II.

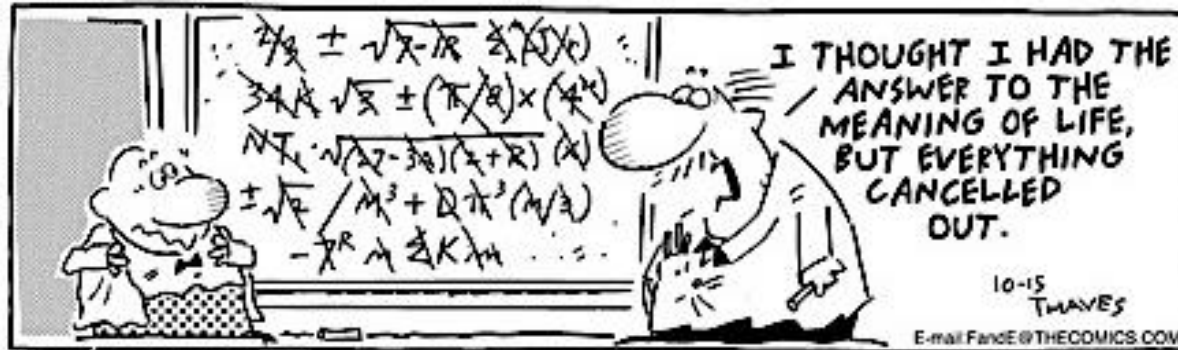
The black points are the position of the resonance in the space $(\Re[s], \Im[s], \Re[J])$. The blue circles are the position of the poles with uncertainties and the blue and red points are the projections of the resonances positions (black points) in the planes $(\Re[s], \Re[J])$ and $(\Im[s], \Re[J])$, i.e. the Chew-Frautschi and the $(\Im[s], \Re[J])$ plots.

Conclusions

- Regge theory imposes important restrictions to the extractions of resonant states.
- We find a signal of physics beyond compact $3q$ picture for $N(1680)$, $N(1720)$ and some members of $\frac{3}{2}^-_{(-)}$ trajectory.
- Exchange degeneracy is clearly broken in the non-strange sector.
- Trajectories $\frac{1}{2}^-$ and $\frac{3}{2}^+$ are poorly known and Regge phenomenology cannot provide insight into the internal structure of the baryons
- The parameters $\frac{1}{2}^+_{(+)}$ (nucleons) y $\frac{3}{2}^-_{(-)}$ (Δ) are estimated as $\alpha' = 0.99 \pm 0.12 \text{ GeV}^{-2}$ and $\alpha' = 1.21 \pm 0.15 \text{ GeV}^{-2}$ respectively; those are compatible with quark model predictions and high energy fits for $p\bar{p}$.
- More information in:

JASC *et al.* *PRD* 99 (2019) 034003 More on: JPAC, *PRL* 123 (2019) 092001

Thank you for your attention



Questions?

Extra slides

N^* Pole parameters

TABLE I. Summary of pole positions M_p , Γ_p in MeV for $I^\eta = \frac{1}{2}^+$ states, where $M_p = \Re[\sqrt{s_p}]$ and $\Gamma_p = -2\Im[\sqrt{s_p}]$. I stands for isospin, η for naturality, J_p for spin, and P for parity. Naturality and parity are related by $\eta = \tau P$, where τ is the signature. For baryons, $\eta = +1$, natural parity, if $P = (-1)^{J_p-1/2}$, and $\eta = -1$, unnatural parity, if $P = -(-1)^{J_p-1/2}$.

Name	$N(939)$	$N(1520)$	$N(1680)$	$N(2190)$	$N(2220)$
Status	****	****	****	****	****
$I^\eta J_p$	$\frac{1}{2}(+) 1/2^+$	$\frac{1}{2}(-) 3/2^-$	$\frac{1}{2}(+) 5/2^+$	$\frac{1}{2}(-) 7/2^-$	$\frac{1}{2}(+) 9/2^+$
CMB	939(1), 0	1510(5), 114(10)	1667(5), 110(10)	2100(50), 400(160)	2160(80), 480(100)
JüBo	939(1), 0	1509(5), 098(3)	1666(4), 081(2)	2084(7), 281(6)	2207(89), 659(140)
BnGa	939(1), 0	1507(3), 111(5)	1676(6), 113(4)	2150(25), 325(25)	2150(35), 440(40)
SAID(SE)	939(1), 0	1512(2), 113(6)	1678(4), 113(3)	2132(24), 550(25)	2173(7), 445(21)
SAID(ED)	939(1), 0	1515(2), 109(4)	1674(3), 114(7)	2060(11), 521(16)	2177(4), 464(9)
KH80	939(1), 0	1506(2), 115(3)	1674(3), 129(4)	...	2127(27), 380(29)
KA84	939(1), 0	1506(2), 116(4)	1672(3), 132(5)	...	2139(6), 390(7)

TABLE II. Summary of pole positions M_p , Γ_p in MeV for $I^\eta = \frac{1}{2}^-$ states. Notation as in Table I.

Name	$N(1720)$	$N(1675)$	$N(1990)$	$N(2250)$
Status	****	****	**	****
$I^\eta J_p$	$\frac{1}{2}(-) 3/2^+$	$\frac{1}{2}(+) 5/2^-$	$\frac{1}{2}(-) 7/2^+$	$\frac{1}{2}(+) 9/2^-$
CMB	1680(30), 120(40)	1660(10), 140(10)	1900(30), 260(60)	2150(50), 360(100)
JüBo	1689(4), 191(3)	1647(8), 135(9)	2152(12), 225(20)	1910(53), 243(73)
BnGa	1670(25), 430(100)	1655(4), 147(5)	1970(20), 250(20)	2195(45), 470(50)
SAID(SE)	1668(24), 303(58)	1661(1), 147(2.4)	2157(62), 261(104)	2283(10), 304(31)
SAID(ED)	1659(11), 303(19)	1657(3), 139(5)	...	2224(5), 417(10)
KH80	1677(5), 184(9)	1654(2), 125(4)	2079(13), 509(23)	2157(17), 412(51)
KA84	1685(5), 178(9)	1656(1), 123(3)	2065(14), 526(9)	2187(7), 396(25)

Δ^* Pole parameters

TABLE III. Summary of pole positions M_p , Γ_p in MeV for $I^\eta = \frac{3}{2}^+$ states. Notation as in Table I.

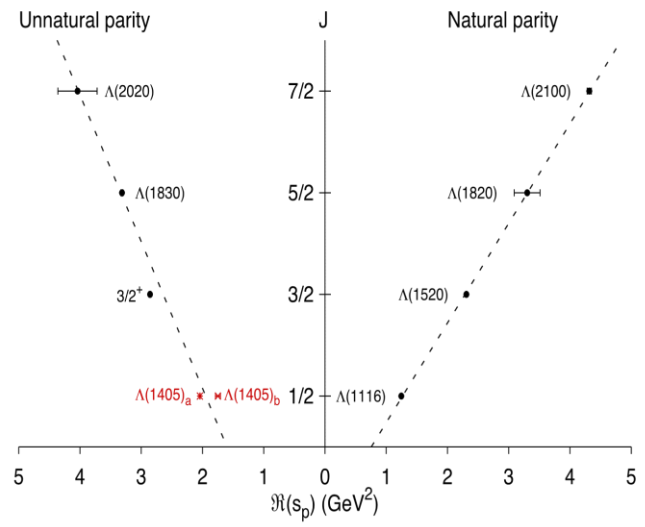
Name	$\Delta(1700)$ ****	$\Delta(1905)$ ***	$\Delta(2200)$ ***	$\Delta(2300)$ **
Status				
$I^\eta J_P^P$	$\frac{3}{2}(-) 3/2^-$	$\frac{3}{2}(+) 5/2^+$	$\frac{3}{2}(-) 7/2^-$	$\frac{3}{2}(+) 9/2^+$
CMB	1675(25), 220(40)	1830(40), 280(60)	2100(50), 340(80)	2370(80), 420(160)
JüBo	1667(28), 305(45)	1733(47), 435(264)	2290(132), 388(204)	...
BnGa	1685(10), 300(15)	1800(6), 290(15)
SAID(SE)	1646(11), 203(17)	1831(7), 329(17)
SAID(ED)	1652(10), 248(28)	1814(5), 273(9)
KH80	1643(9), 217(18)	1752(5), 346(8)
KA84	1616(5), 280(9)	1790(5), 293(12)

TABLE IV. Summary of pole positions M_p , Γ_p in MeV for $I^\eta = \frac{3}{2}^-$ states. Notation as in Table I.

Name	$\Delta(1232)$ ****	$\Delta(1930)$ ***	$\Delta(1950)$ ****	...	$\Delta(2420)$ ****
Status					
$I^\eta J_P^P$	$\frac{3}{2}(-) 3/2^+$	$\frac{3}{2}(+) 5/2^-$	$\frac{3}{2}(-) 7/2^+$	$\frac{3}{2}(+) 9/2^-$	$\frac{3}{2}(-) 11/2^+$
CMB	1210(1), 100(2)	1890(50), 260(60)	1890(15), 260(40)	...	2360(100), 420(100)
JüBo	1215(4), 97(2)	1663(43), 263(76)	1850(37), 259(61)	1783(86), 244(194)	...
BnGa	1210.5(1.0), 99(2)	...	1888(4), 245(8)
SAID(SE)	1211(0), 100(2)	1845(31), 174(40)	1888(3), 234(6)
SAID(ED)	1211(2), 98(3)	1969(23), 248(36)	1878(4), 227(6)	1955(24), 911(24)	2320(13), 442(23)
KH80	1211(2), 98(3)	1848(28), 321(24)	1877(3), 223(5)	...	2454(15), 462(58)
KA84	1210(2), 100(2)	1844(36), 334(26)	1878(3), 246(7)	...	2301(7), 533(17)

Chew-Frautschi and $(\Im[s_p], \Re[J] = J_P)$ (strange sector)

Λ^*



Σ^*

